Int. J. Chem. Sci.: 10(3), 2012, 1277-1292
ISSN 0972-768X
www.sadgurupublications.com

QUANTUM-CHEMICAL SIMULATIONS ON PYRAZOLO [3,4-b] QUINOLINE AS A DOPANT IN MULTIPLAYER-OLED *(Organic Light Emitting Diode)* FABRICATION

N. NADEEM AFROZE* and K. SUBRAMANI

P.G & Research Department of Chemistry, Islamiah College, Vaniyambadi, VELLORE (T.N.) INDIA

ABSTRACT

A series pyrazolo derivatives were used as a dopant in the multiplayer OLED fabrication. The theoretical calculations are done through DFT (density functional theory) method; used to calculate the maximum excitation wavelength (λ^{abs}_{max}) and fluorescence wavelengths (λ_{emi}) of a series of pyrazolo derivatives based on their optimized structures. The substitution effects of PAQ derivatives with electron-withdrawing and electron-donating substituent were investigated according to their photo-physical properties and electroluminescent layers. The calculated DT/DFT/B3LYP/6-31G* had the better linear relationship between them. Presumably, the procedures of theoretical calculation would be employed to predict the electroluminescence characteristics of the other material, and could give a possible way to design novel material for organic light emitting diode as dopant.

Key words: Pyrazolo derivatives, DFT, OLED, Emissive electroluminescent excitation.

INTRODUCTION

A new ultra low-cost, light weight and flexible display technology, based on organic light emitting diodes (OLEDs) is emerging in the field of Chemistry, Physics and material science[1,2]. Since the initial works had been done on the small molecule by Tang et al.[3], and on the polymers by Friend et al.[4], lots of organic compounds were synthesized and applied to the OLED devices for commercial applications. The organic compound contains pyrazoline moiety, which has been explored for emitting layer and hole transporting material in the OLEDs. Huang et al.[5] proposed the pyrazoline derivatives, which could be used in OLED as emitting material. Tao et al.[6-8], used the diprazolopyridine derivatives as efficient blue light-emitting material in multilayer OLED[9,10]. They also reported that diethylamino-substituted pyrazoloquinoline could generate a sharp green electroluminence studied on the photo-

*Author for correspondence; E-mail: nadinfo@gmail.com

physical properties of pyrazolo[3,4-b] quinoline (PAQ) derivatives, which could be the dopants in the polymer-LED materials[11]. In general, the characteristics of PAQ derivatives have the fluorescence wavelengths (λ_{emi}) in blue and bluish-green region and 1 methyl- 3-phenyl-1H-pyrazolo [3,4-b] quinolines (PAQ derivatives) carry different substituents have been synthesized by Tao's group as emitting material (Fig. 1)[12]. According to experimental data, the blue emission has been achieved with these PAQ derivatives as the dopant, in a device of structure: ITO/NPB/CBP/TPBI:PAQ-X/TPBI/ Mg:Ag, where the PAQ-X is 1-methyl-3-phenyl-1H-pyrazolo [3,4-b] quinoline carrying various substituents, CBP is 4,4'-bis [N-(1-naphthyl)-N-phenylamino] biphenyl (α-NPB) and 4,4'-dicarbozolyl-1,1'-biphenyl as hole- transporting materials and TPBI is 2,2',2"-(1,3,5-phenylene)- tris [1-phenyl-1H-benzimidazole] as electron transporting material. Recently, Niziol et al.[13], have proposed the optical properties of a series of PAQ derivatives. They indicated that these pyrazolo derivatives have high quantum efficiency of emission.

Organic light emitting diodes (OLED) are currently investigating a unique application for next generation technologies. Theoretical calculation methods are useful for generating their electronic and geometric structures, absorption and emission spectra. Wang et al.[14], used the semi-empirical AM1 and ab initio DFT methods to determine the electronic transition energies and relative intensities (oscillator strengths) for 1,4-distyrylbenzene (DSB)[15], pyrene and their derivatives. Kooecieñ et al.[16], presented the experimental data and the semiempirical PM3 and AM1 calculations for the PAQ derivatives[17]. The comparison of measured and calculated absorption spectra by semiempirical AM1 method manifested rather good agreement for the PAQ derivatives, with three substituted radicals R_1, R_2, R_3 = methyl or phenyl groups (Fig. 1). In the present work, the Ab initio, DFT B3LYP and the semiempirical AM1 methods were used for generating the geometrical and electronic structures, electronic transition energies (excitation and fluorescence) and relative intensities (oscillator strengths, f) for PAQ and its derivatives.

Our calculations are parameter-free and used in current implementations for DFT energies were calibrated based on the experimental data for these derivatives. The substituents and substitution position effects in PAQ derivatives were also investigated. In particular, the substitution position can be in five positions of the pyrazolo derivatives (Fig. 1).

The computational chemistry simulations can be used as a model system for understanding the relationship between luminescence and molecular structure for these pyrazolo derivatives as electron dopant.

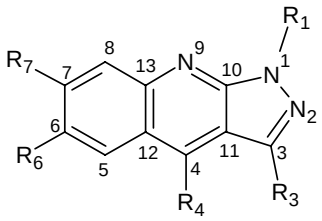

Pyrazoloquinoline (PAQ)

Fig. 1: Five substituent position of PAQ

Computational studies

The molecular geomentries of PAQ derivatives under computational studies are calculated through, Ab initio DFT, B3LYP, with 6-31G* basis set and the semiempirical AM1 and PM3 methods were used for optimization of PAQ structures and its derivatives. Comparing the calculated results, the calculated geometrical parameters of PAQ (Table 1) by Ab initio RHF/6-31G* and DFT B3LYP/ 6-31G* calculations. Due to the computing time limitations, have the similar results with those of the semiempirical AM1 and PM3 calculations. Due to the computing time limitation, the optimized structures of PAQ derivatives were determined by using the semiempirical AM1 and Ab initio DFT B3LYP methods for every calculation. The electronic transition properties, which include the maximum excitation wavelength (λ^{abs}_{max}) and relative intensities (oscillator strengths, *f*), were obtained by the semiempirical ZINDO method and Time Dependent Density Functional Theory (TD-DFT), respectively. These calculations were based on the optimized structures by DFT and AM1 methods and referred as "TD-DFT/method" or "ZINDO/method". The keyword "EXICTED" was used for the optimized structure of the excited state (S_1).

Table 1: Calculated bond lengths (Å) of optimized PAQ*

Bond length	HF/ 6-31G*	B3LYP/ 6-31G*	AM1	PM3
N1-N2	1.360	1.361	1.332	1.372
N2-C3	1.270	1.316	1.347	1.332
C3-C11	1.460	1.438	1.468	1.442
C11-C4	1.350	1.386	1.369	1.372
C4-C12	1.410	1.419	1.411	1.414
C12-C5	1.440	1.428	1.423	1.429
C5-C6	1.360	1.372	1.364	1.360
C6-C7	1.440	1.426	1.415	1.424

Cont…

Bond length	HF/ 6-31G*	B3LYP/ 6-31G*	AM1	PM3
C7-C8	1.360	1.375	1.367	1.361
C8-C13	1.410	1.422	1.444	1.431
N9-C13	1.350	1.353	1.373	1.372
N9-C10	1.320	1.312	1.331	1.342
C10-N1	1.320	1.361	1.412	1.402
C10-C11	1.427	1.436	1.479	1.441
C12-C13	1.490	1.442	1.433	1.422

*The molecular structure of PAQ is described in Fig. 1.

The computational calculated fluorescence wavelengths (λ_{emi}) and relative intensities (oscillator strengths, f) were determined by ZINDO calculations based on the optimized excited state structure, which was obtained from the AM1 calculation, we named it as ZINDO/AM1 for this calculation. In this study, the vertical excited upward transition from the optimized structure in the excited state (S_1) equals the downward vertical fluorescence transition (S_0-S_1). The excitation energy calculations in this paper were limited to the first excited electronic state corresponding to the HOMO-LUMO single excitation. The semiempirical ZINDO, AM1, and Ab initio DFT and TD-DFT calculations were performed employing the MOPAC 2000[18] and Gaussian 03 packages[19], respectively. In this study, thirty PAQ derivatives in Fig. 2 were investigated by the semiempirical AM1 method and Ab initio DFT B3LYP method with the basis of 6-31G* for the optimization and it properties.

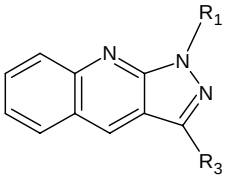

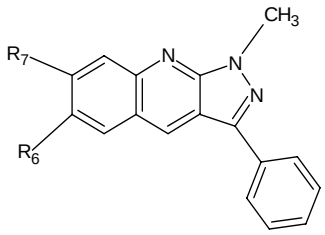

1. R_1-Me,R_3-H
2. R_1 = H,R_3=Me
3. R_1= Me,R_3=Me
4. R_1=Me,R_3=Ph
5. R_1=Ph,R_3=Me
6. R_1=Ph,R_3=Ph

18. R_6=Me,R_7=H
19. R_6 = OMe,R_7=H
20. R_6= F,R_7=H
21. R_6=CN,R_7=H
22. R_6=Net_2,R_7=H
23. R_6=t-Bu,R_7=H
24. R_6=H,R_7=CF_3

Cont…

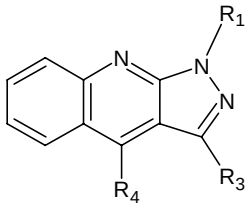

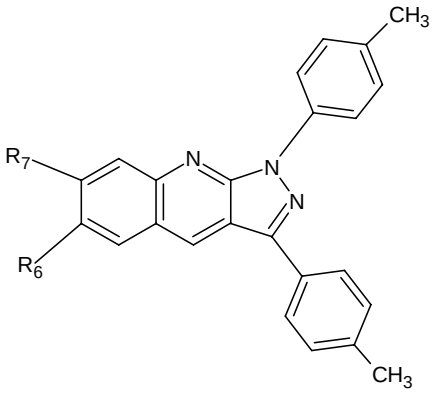

7. R_1=Ph,R_3=Me,R_4=Me
8. R_1=Ph, R_3=Ph,R_4=Me
9. R_1=Me,R_3=Me,R_4=Ph
10. R_1=Me,R_3=Ph,R_4= Ph
11. R_1=Ph,R_3=Me, R_4=Ph
12. R_1=Ph,R_3=Ph, R_4= Ph
25. R_6=H,R_7=H
26. R_6 = F,R_7=H
27. R_6= OMe,R_7=H
28. R_6=CN,R_7=H
29. R_6= t-Bu,R_7=H

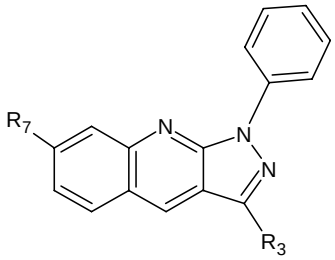

13. R_3=Et,R_7=H
14. R_3 = *n*-Pr,R_7=H
15. R_3= *n*-Bu,R_7=H
16. R_3= *t*-Bu,R_7=H
17. R_3=*t*-Bu,R_7=H

Fig. 2: Molecular structure of PAQ derivatives

RESULTS AND DISCUSSION

Calculated maximum excitation wavelength of PAQ and its derivatives

In Figure-2 the molecular structures of PAQ and its derivatives are shown. In order to study the substituents effect in mono-substituted PAQ compound, different substituents

were added with five substitution positions of PAQ (Fig. 1). Since these related PAQ derivatives have been proposed by the experimental work, calculated maximum excitation wavelength (λ^{abs}_{max}) and fluorescence wavelengths (λ_{emi}) as well as related experimental data for these PAQ derivatives were shown in Table 2. Fabian and Co-workers suggested that compounds with low extinction coefficient (≈6000 l mol^{-1} cm^{-1}) also had low oscillator strength (< 0.3), whereas those with high extinction coefficient (≈15000 l mol^{-1} cm^{-1}) were characterized by oscillator strength (*f*) ≥ 0.5 compound[20,21]. In particular, the maximum excitation wavelength (λ^{abs}_{max}) were dominated by the HOMO-LUMO single excitation and their extinction coefficients (oscillator strength, *f*) distinguished the peak of excited electronic state transition with its maximum range of about 350 nm to 420 nm, which were generated by the highest of the oscillator strengths distinguished the peak of excited electronic state transition in the PAQ derivatives. In this work, several different calculated methods were used to calculate the maximum excitation wavelength (λ^{abs}_{max}) for PAQ and its derivatives. To generate a better calculated method in this study, we plot the experimental excitation and emission wavelength *vs.* calculated maximum excitation wavelength (λ^{dbs}_{max}) and fluorescence wavelength (λ_{emi}), which are shown in Fig. 3, 4, 5 and 6. In the experiment, the spectra of compounds 13-18 were measured with ethyl acetate and others are with chloroform. The experimental excitation wavelength and emission wavelength of compounds 13-18 were as shown in Fig. 3, 4, 5 and 6.

The corresponding regression equations were given as follows:

$\lambda_{Exp} = 0.7466\lambda_{cal} + 127.41$, $r^2 = 0.8603$ (ZINDO/AM1)

$\lambda_{Exp} = 1.1328\lambda_{cal}-14.782$, $r^2 = 0.9014$ (ZINDO/DFT)

$\lambda_{Exp} = 2.3414\lambda_{cal} -503.56$,$\rho^2 = 0.9288$ (TD/DFT for excitation wavelength)

$\lambda_{Exp} = 0.9324\lambda_{cal} + 109.77$, $r^2 = 0.8454$ (ZINDO/AM1 for fluorescence wavelength)

Where λ_{Exp} and λ_{cal} are the experimental excitation wavelength and the calculated maximum excitation wavelength (or fluorescence wavelength), respectively. r^2 is the correlation coefficient. According to the above calculation results, the calculated excitation wavelength with TD/DFT method has the higher correlation coefficient r^2 (> 0.92) and generating the better linear relationship than other calculation results with experimental data. The errors were around ±40 and ±85 nm for excitation and fluorescence wavelengths, respectively.

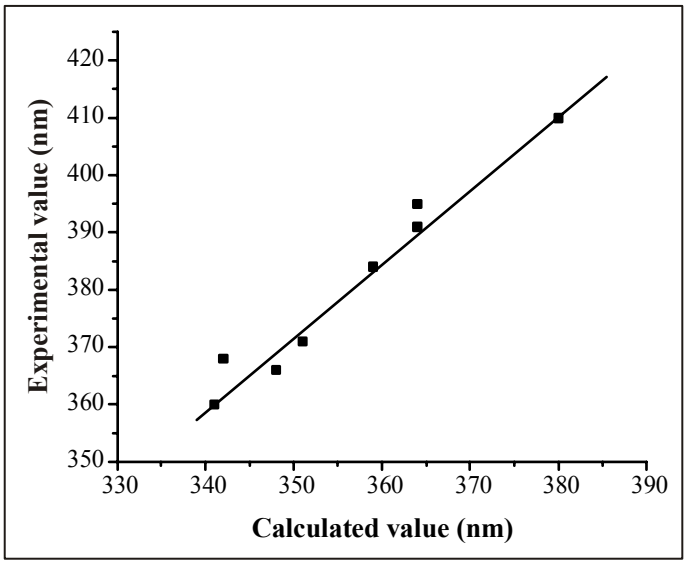

Fig. 3: Plot of calculated maximum excitation wavelength (λ^{abs}_{max}) (ZINDO/AM1 method) vs. experimental absorption

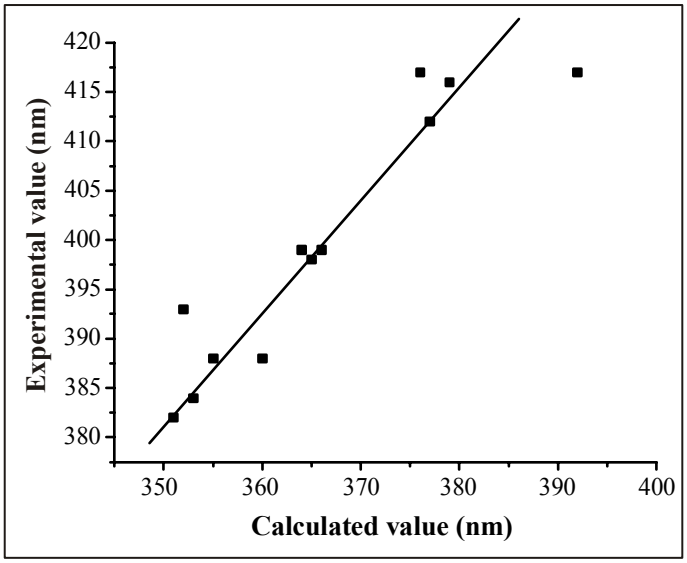

Fig. 4: Plot of calculated maximum excitation wavelength (λ^{abs}_{max}) (ZINDO/DFT method) vs. experimental absorption

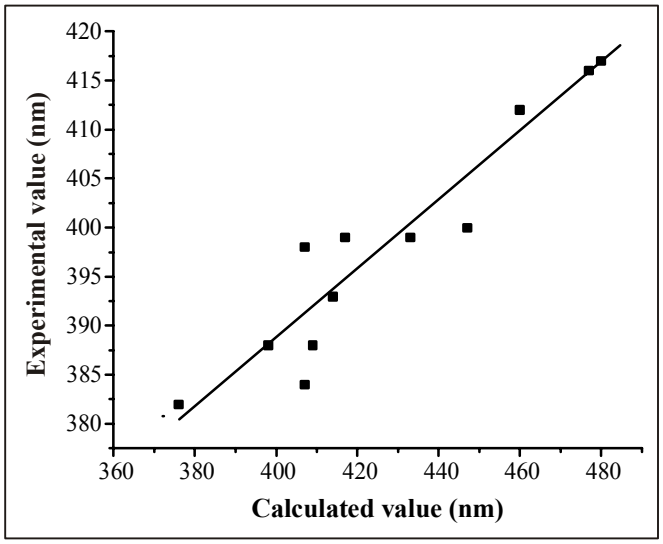

Fig. 5: Plot of calculated maximum excitation wavelength (λ^{abs}_{max}) (TD/DFT method) vs. experimental absorption

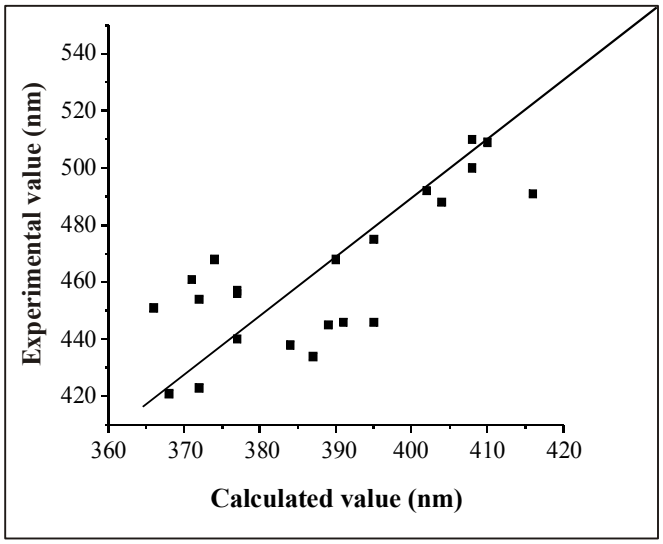

Fig. 6: Plot of calculated florescence wavelength vs. experimental absorption

Substitution position effect in PAQ derivatives

Theoretical investigation on PAQ derivatives, the methyl and phenyl substitutes at 1, 3 and 4 positions of PAQ (Fig. 1) were proposed. Ab initio DFT/B3LYP/6-31G* and TD/DFT/B3LYP/6-31G* calculations were used to determine the orbital energies of HOMO,

LUMO and maximum excitation wavelength (λ^{abs}_{max}) for these PAQ derivatives (Table 2). Since methyl and phenyl substituents are electrondonating groups, they push the electron to the PAQ moiety and increase the π electron density. The orbital energy of HOMO increased more than that of LUMO for PAQ derivatives with the methyl and phenyl group at 1, 3 and 4 substitutions. Thus, the excitation energies and the HOMO-LUMO energy gap of PAQs derivatives would decrease except the substituents at position 4. The calculated results show that the PAQ with the methyl and phenyl groups generate the red-shifted excitation wavelength comparing to the PAQ without any substituent. The 4-substituted PAQ (except compounds 9 and 11) decrease the excitation energy and generate the blue-shifted excitation wavelength comparing to PAQ. We compared the calculated results for two sets of compounds 3, 5, 9 and 11. All of them are 1,3 substituted PAQ with methyl and phenyl substituents and without 4-substitution for compounds 3 and 5. According to Table 2, compounds 3 and 5, (1,3 substituted PAQ) have blue-shifted calculated maximum excitation wavelength to those of compounds 9, 11 (1, 3, 4 substituted PAQ). Since compounds 9 and 11 have 4-substitution in PAQ and it may cause the steric effect in these PAQ derivatives. Comparing the optimized structures of compounds 9-12, which are the substituted 1, 3 & 4. PAQ and the methyl group at 3-substitution, the dihedral angle (α) is between PAQ moiety and the phenyl substituents for 4-substitution increasing due to the Steric effect. The calculated dihedral angle (α) at compounds 11 and 12 is 75.3º and 64.2º, respectively. The calculated results (Table 2) indicated that the substitution position effect increases as the following: 1- > 3- in the PAQ derivatives. For the maximum excitation wavelength (λ^{abs}_{max}) of PAQ derivatives, 3-phenyl PAQ has higher oscillator strength than that of the methyl substituted or unsubstituted PAQ.

Table 2: Calculated maximum excitation wavelength ((λ^{abs}_{max}, nm) (by ZINDO/AM1, ZINDO/DFT/6-31G*and TDDFT/ B3LYP/6-31G*), fluorescence (λ_{emi}, nm) (by ZINDO/AM1) as well as the experimental excitation wavelength {(λ^{abs}_{max}, nm) and fluorescence λ_{emi}, nm} of PAQ and its derivatives

Cpda	Calculated value				Experimental value	
	ZINDO/AM1[b]		ZINDO/DFT[c]	TD-DFT[c]		
	λ^{abs}_{max}	λ_{emi}	λ^{abs}_{max}	λ^{abs}_{max}	λ^{abs}_{max}	λ_{emi}
PAQ	341	360	346	346	-	-
1	343	362	350	358	-	-
2	336	359	346	352	-	-
3	346	363	352	366	-	-

Cont…

Cpda	Calculated value				Experimental value	
	ZINDO/AM1*b*		ZINDO/DFT*c*	TD-DFT*c*		
	λ^{abs}_{max}	λ_{emi}	λ^{abs}_{max}	λ^{abs}_{max}	λ^{abs}_{max}	λ_{emi}
4	359	384	360	398	388[d]	437[d]
5	351	372	355	409	387[d]	456[d]
6	367	390	366	433	399[d]	467[d]
7	350	371	355	409	-	-
8	351	371	355	409	388[e]	464[e]
9	351	371	355	409	388[e]	463[e]
10	352	372	355	409	-	-
11	360	377	363	413	388[e]	453[e]
12	348	366	353	407	384[e]	457[e]
13	345	377	357	415	390[e]	458[e]
14	338	372	351	376	382[d]	425[d]
15	338	377	355	393	388[d]	451[d]
16	342	368	352	414	393[d]	452[d]
17	339	374	353	426	400[d]	463[d]
18	365	387	366	397	-	-
19	368	389	371	403	412[f]	444[f]
20	364	391	365	407	398[f]	446[f]
21	363	395	363	421	398[f]	469[f]
22	377	408	392	447	451[f]	522[f]
23	365	387	366	396	388[f]	433[f]
24	364	395	364	417	399[f]	447[f]
25	375	401	371	448	-	-
26	381	408	377	460	412[d]	502[d]
27	379	402	379	460	417[d]	491[d]
28	380	410	376	480	417[d]	532[d]
29	379	404	376	451	407[d]	489[d]
30	384	416	379	477	416[d]	492[d]

[a]The molecular structures of PAQ and its derivatives are shown in Fig. 2b. The

geometries of PAQ and its derivatives were optimized by AM1. c The geometries of PAQ and its derivatives were optimized by DFT(B3LYP /6-31G*). [d] Ref.[22], [e] Ref.[23], [f] Ref.[24].

Substituent effect in PAQ derivatives

The effect of given substitution position effect, we used the DFT B3LYP and TD/DFT/B3LYP calculation method to determine the HOMO, LUMO orbital energies and the maximum excitation wavelength (λ^{abs}_{max}) of PAQ derivatives with different substituents. Table 4 shows the calculated molecular orbital energies of HOMO and LUMO for these PAQ derivatives. Compounds 5 and 13-16 are different alkyl substituents at 3-substituted PAQ (Fig. 1). There are similar calculated HOMO and LUMO orbital energies and the energy gap (ΔE) for these PAQ derivatives. The differences of the calculated energy gap (ΔE) (0.131 eV, 0.131 eV, 0.132 eV, 0.132 eV and 0.131 eV) of methyl, ethyl, propyl, n-butyl and *t*-Butyl substituents at the 3-substituted PAQ derivatives are very small. In order to investigate the influences of different substituents at the 6-substituted PAQ derivatives, -F, -CN electron withdrawing and -Me, -OMe, -NEt_2,*t*-Butyl, electron-donating substituents were used for these PAQ derivatives (Compounds 18-23 and 25-29, Fig. 1).The calculated HOMO, LUMO and the maximum excitation wavelength (λ^{abs}_{max}) for these PAQ derivatives were calculated by Ab initio DFT and TD/DFT method, the calculation results are shown in Tables 2 and 5. The electron-withdrawing group reduced the p-electron density in the parent PAQ ring. Thus, both the orbital energies of HOMO and LUMO were decreasing by the electron-withdrawing substituent in the PAQ derivatives. According to the electronic structure analysis, the orbital energy of LUMO decreased much more than that of HOMO in the PAQ derivatives with the electron- withdrawing substituent at the 6-position and the energy gap (ΔE = LUMO – HOMO) of them would decrease. Thus, the electron-withdrawing substituent resulted in a red-shifted excitation wavelength to the non-substituent at the 6-position of PAQ (compound 4 *vs.* compounds 20-21 and compound 25 *vs.* compounds 26, 28). The substituent effect in the PAQ derivatives with the electron-withdrawing substituent at the 6-position has the following order: -CN > -F.

In the contrast, the PAQ derivatives with electron- donating substituent increased the π electron density in the PAQ moiety, and the orbital energies of HOMO and LUMO increases.

According to electronic structure examination, the orbital energy of LUMO increases much more than that of HOMO in compounds 18 and 23 and their energy gap (ΔE) increase. The electron- donating substituent resulted in a blue-shift excitation wavelength to the non-substituent at the 4-position of PAQ (compounds 4 *vs.* compounds 18 and 23), but the results of compounds 19 (6-OCH_3-PAQ) and 22 (6-NEt_2-PAQ) were just the opposite.

The orbital energy difference of LUMO between compounds 4 and 19 or 22 was larger than that of compounds 4 and 18 or 23 are electrons donating substituents.

Table 3: DFT/B3LYP/6-31G* calculated HOMO (eV), LUMO (eV) and ΔE (= LUMO – HOMO) (eV) for the 1-, 3-, 4-substituted PAQ

Cpd$_a$	DFT		
	HOMO	LUMO	ΔE
PAQ	-0.215	-0.068	0.147
1	-0.209	-0.066	0.144
2	-0.210	-0.065	0.146
3	-0.205	-0.063	0.142
4	-0.201	-0.069	0.131
5	-0.201	-0.070	0.131
6	-0.199	-0.075	0.124
7	-0.198	-0.067	0.131
8	-0.198	-0.070	0.129
9	-0.200	-0.062	0.138
10	-0.199	-0.067	0.133
11	-0.198	-0.068	0.130
12	-0.215	-0.068	0147

According to the electronic structure analysis, the mixing of the lone pair electrons on the nitrogen or oxygen into the HOMO orbital would raise the HOMO level more and decrease the energies gap (Δ*E*).

Table 4: DFT/B3LYP/6-31G* calculated HOMO (eV), LUMO (eV) and ΔE (= LUMO – HOMO, eV) for the 3- alkyl PAQ

Cpd$_a$	DFT		
	HOMO	LUMO	ΔE
5	-0.202	-0.070	0.131
13	-0.201	-0.069	0.131
14	-0.0200	-0.069	0.132
15	-0.200	-0.069	0.132
16	-0.201	-0.069	0.131

[a]: The molecular structures of the derivatives are shown in Fig. 2.

The electron-donating substituent resulted a red-shift excitation wavelength as compared to the PAQ derivatives without any R_4 substitution (compound 4 *vs.*19 and compound 25 *vs.* 27). The substituent effect in the PAQ derivatives with the electron-withdrawing/donating substituent at the 6- position has the follow order:

$-NEt_2$ > -CN > -F > -OMe > *t*-Butyl ≈ -Me.

Table 5: DFT/B3LYP/6-31G* calculated HOMO (eV), LUMO (eV) and ΔE (= LUMO HOMO, eV) for the 6-, 7- substituted PAQ

Cpd[a]	DFT		
	HOMO	**LUMO**	**ΔE**
5	-0.202	-0.070	0.131
13	-0.201	-0.069	0.131
14	-0.0200	-0.069	0.132
15	-0.200	-0.069	0.132
16	-0.201	-0.069	0.131

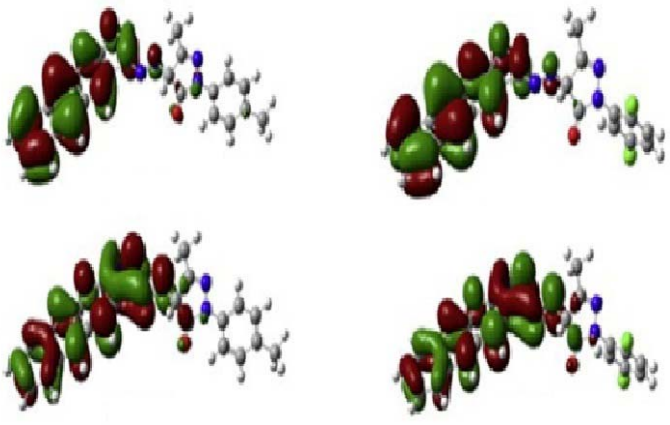

HOMO **LUMO**

Fig.7 Calculated HOMO, LUMO

CONCLUSION

The performed molecular dynamics simulation of PAQ derivatives could be used as dopants in the multi-layer OLED fabrication. In this study, the maximum excitation wavelength (λ^{abs}_{max}) was calculated by Ab initio TD-DFT and the semiempirical ZINDO methods. These calculated data generated an excellent agreement with the linear relationship between experimental and calculated absorption (λ^{abs}_{max}) than by the calculated ZINDO/AM1 method. We used the Ab initio DFT and TD-DFT calculated methods to investigate the substitution position effect and substituents effect in the PAQ derivatives. The maximum excitation wavelength (λ^{abs}_{max}) of PAQ derivatives with the methyl and phenyl substituents have red-shifted excitation wavelength to the PAQ derivatives without 1- and 3- substitution; the substitution position effect for these PAQ derivatives increase in the following order 1- > 3. Besides, the 3-phenyl-PAQ has higher oscillator strength than that of the 3-methyl PAQ both for the calculations and experimental work. 4-methyl-PAQ, and 4-phenyl-PAQ have the blue-shifted excitation wavelength to the PAQ derivatives with non-substituent at the 4-position of PAQ except 3-methyl-4-phenyl-PAQ. 3-alkyl-PAQ with different alkyl group generates a smaller substituent effect than that of PAQ compound. For 6-substituted PAQ, the electron-withdrawing substituent determined as a red-shifted excitation wavelength to the non-substituent at the 6-position of PAQ. Except compounds 19(6-OCH_3-PAQ) and 22 (6-NEt_2-PAQ), electron- donating substituent resulted in a blue-shifted excitation wavelength to PAQ compound. Actually, most of the above calculations result has been confirmed by the related experimental data. Computational Chemistry methods have proven to be a useful tool in all the cases presented in this work. As such, they can be used to aid design of new optically active material in future research in the field of both linear and non linear optics as well as sensors.

ACKNOWLEDGMENT

The first author is thankful to Vaniyambadi Muslim Educational Society for providing necessary facilities to carryout this research work.

REFERENCES

1. A. P. De Silva, H. Q. N. Gunaratne, T. Gunnlaugsson, A. J. M. Huxley, C. P. McCoy, J. T. Rademacher and T. E. Rice, Chem. Rev., **97**, 1515 (1997).

2. C. E. Kerr, C. D. Mitchell, J. Headrick, B. E. Eaton and T. L. Netzel, J. Phys. Chem. B, **104**, 1637 (2000).

3. C. W. Tang and S. A. VanSlyke, Appl. Phys. Lett., **51** (1987) p. 913.

4. J. H. Burrounghs, D. D. C. Bradley, A. R. Brown, R. N. Marks, K. Mackey, R. H. Friend, P.L. Burns and A. B. Holmes, Nature, **347** (1990) p. 359.

5. X. C. Gao, H. Gao, L. Q. Zhang, B. W. Zhang, Y. Gao and C. H. Huang, J. Mater. Chem., **9** p. 1077.

6. E. Balasubramanian, Y. T. Tao, A. Danel and P. Tomasik, Chem. Mater., **12** (2000) p. 2000.

7. Y. T. Tao, E. Balasubramanian, A. Danel and P. Tomasik, Appl. Phys. Lett., **77**, (2000) p. 933.

8. Y. T. Tao, E. Balasubramanian, A. Danel, B. Jarosz and P. Tomasik, Appl. Phys. Lett., **77**, (2000) p. 1575.

9. P. M. Borsenberger and L. B. Schein, J. Phys. Chem., **98** (1994) p. 233.

10. R. H. Young and J. J. Fitzgerald, J. Phys. Chem., **99**, 4230 (1995).

11. M.J.S.Dewar, E.F.Healy, and J.J.P. Steward, J.Comput.Chem.,(1984)5,358

12. Y. T. Tao, E. Balasubramanian, A. Danel, B. Jarosz and P. Tomasik, Chem. Mater., **13** (2001) p. 1207.

13. J. Niziol, A. Danel, G. Boiteux, J. Davenas, B. Jarosz, A. Wisla and G. Seytre, Synth. Met., **127** (2002) p. 175.

14. B. C. Wang, J.-C. Chang, J.-H. Pan, C. Xue and F.-T. Luo, J. Mol. Struct., 636 (2003) p. 81.

15. Z. He, G. H. W. Milburn, K. J. Baldwin, D. A. Smith, A. Danel and P. Tomasik, J. Lumin., **86** (2000) p. 1.

16. E. Kooecieñ et al., / Optics Communications, **227**, 115–123 (2003).

17. R. Chang, J. H. Hsu, W. S. Fann, K. K. Liang, C. H. Chang, M. Hayahshi, J. Yu, S. H. Lin, E. C. Chang, K. R. Chuang and S. A. Chen, Chem. Phys. Lett., **317** (2000) p. 142.

18. Jimmy. James. P. Steward, Fujustu Limted, Tokyo, Japan (2000).

19. M. J. Frisch, G. W. Trucks, H. B. Schlegel, G. E. Scuseria, M. A. Robb, J. R. Cheeseman et al., Chem. Phys. Lett., **317** (2000) p. 142.

20. W. M. F. Fabian, K. S. Niederreiter, G. Uray and W. Stadlbauer, J. Mol. Struct., 477 (1999) p. 209.

21. W. M. F. Fabian and J. M. Kauffman, J. Lumin., **85** (1999) p. 137.

22. R. Chang, J. H. Hsu, W. S. Fann, K. K. Liang, C. H. Chang, M. Hayahshi, J. Yu, S. H. Lin, E. C. Chang, K. R. Chuang and S. A. Chen, Chem. Phys. Lett., **317** (2000) p. 142.

23. L. Hennig, T. M€uller and M. Grosche, J. Prakt. Chem., **332**, 693 (1990).

24. J. Yu, W. S. Fann and S. H. Lin, Theor. Chem. Acc., **103** (2000) p. 374

Revised : 15.05.2012 *Accepted : 18.05.2012*